

Supporting Information for

**High-Quality Metal Oxide Core/Shell Nanowire Arrays on Conductive Substrates for
Electrochemical Energy Storage**

Xinhui Xia,^{†‡} Jiangping Tu,^{†,*} Yongqi Zhang,[†] Xiuli Wang,[†] Changdong Gu,[†] Xinbing Zhao,[†]

and Hong Jin Fan^{†,*}

[†] State Key Laboratory of Silicon Materials and Department of Materials Science and
Engineering, Zhejiang University, Hangzhou 310027, China

[‡] Division of Physics and Applied Physics, School of Physical and Mathematical Sciences,
Nanyang Technological University, Singapore 637371, Singapore

E-mail address: fanhj@ntu.edu.sg; tujp@zju.edu.cn

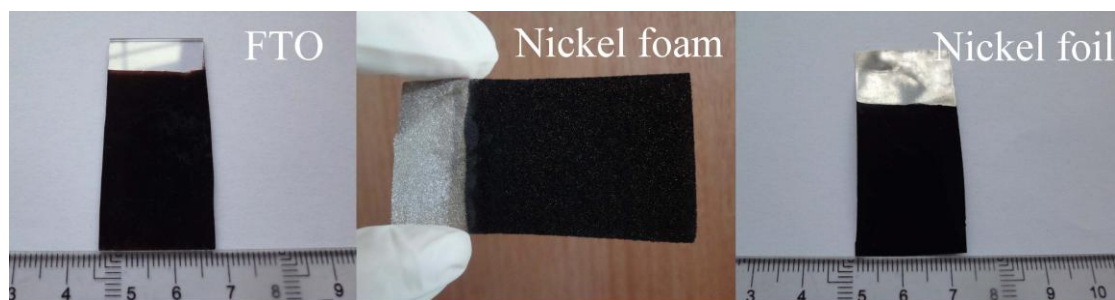


Figure S1. Photographs of Co₃O₄/NiO core/shell nanowire arrays grown on FTO glass, nickel foam and nickel foil substrates.

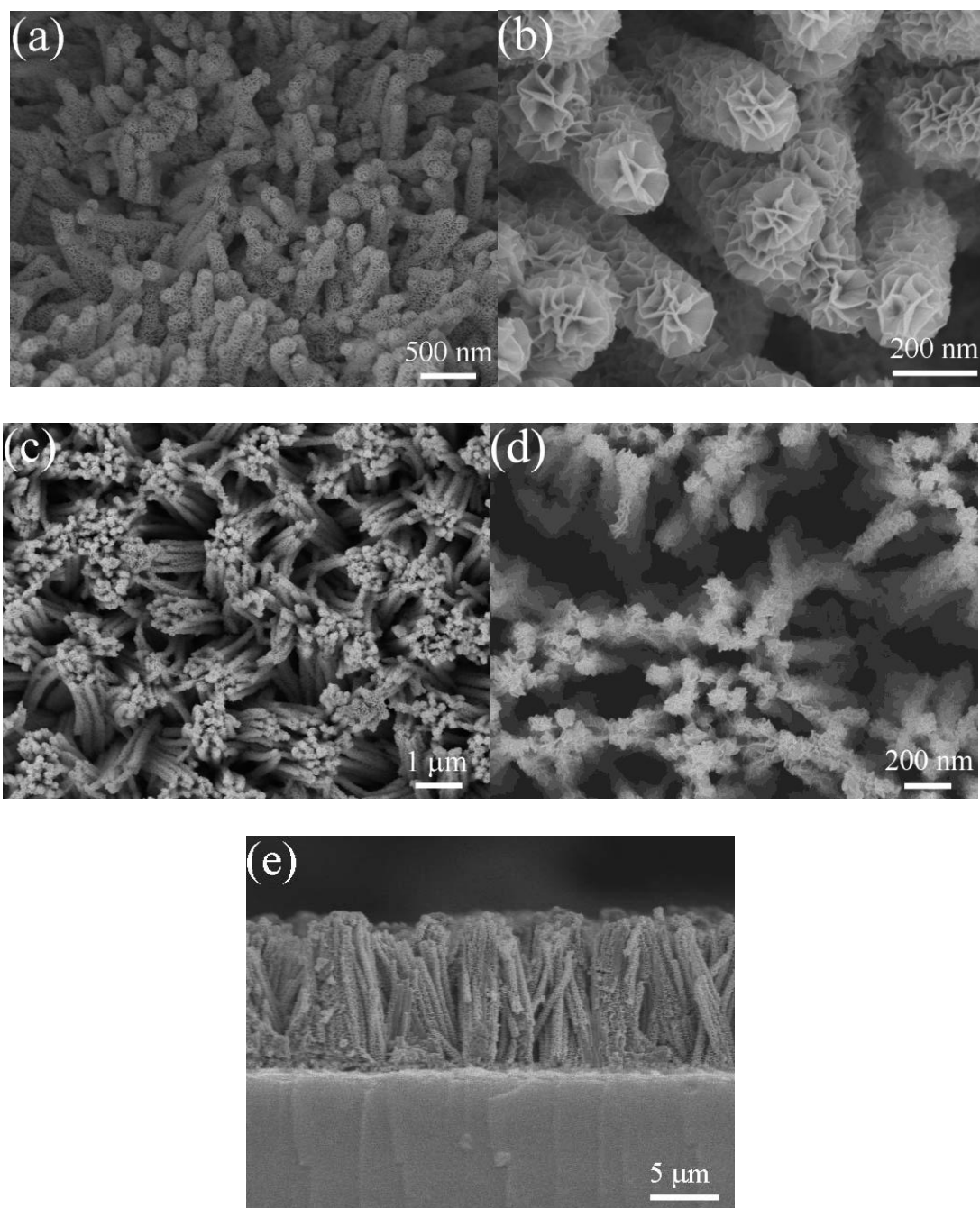


Figure S2. $\text{Co}_3\text{O}_4/\text{NiO}$ core/shell nanowire arrays on different substrates. (a, b) nickel foam and (c, d) nickel foil substrates. (e) Side view of $\text{Co}_3\text{O}_4/\text{NiO}$ core/shell nanowire array.

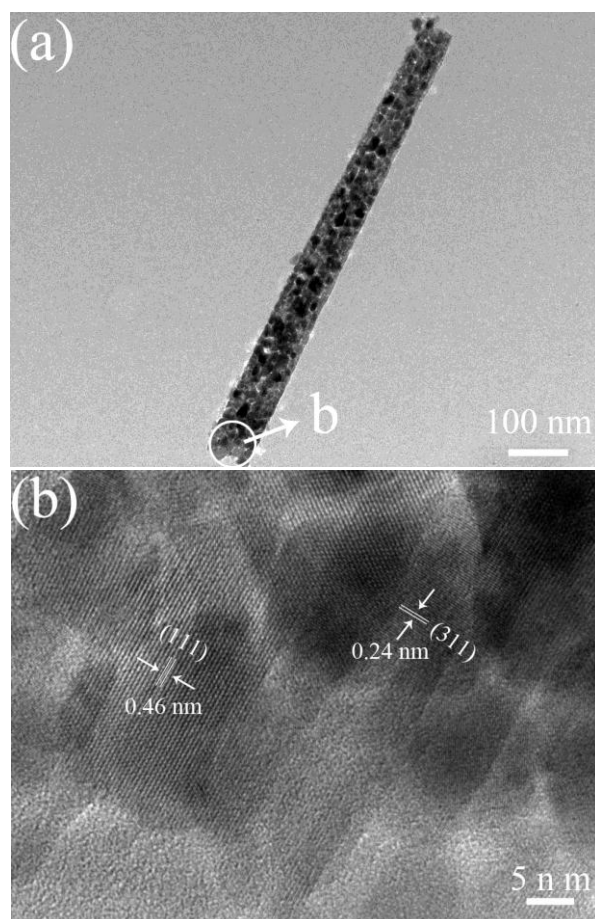


Figure S3 (a) TEM and (b) HRTEM images (magnified region in b) of the Co_3O_4 nanowire.

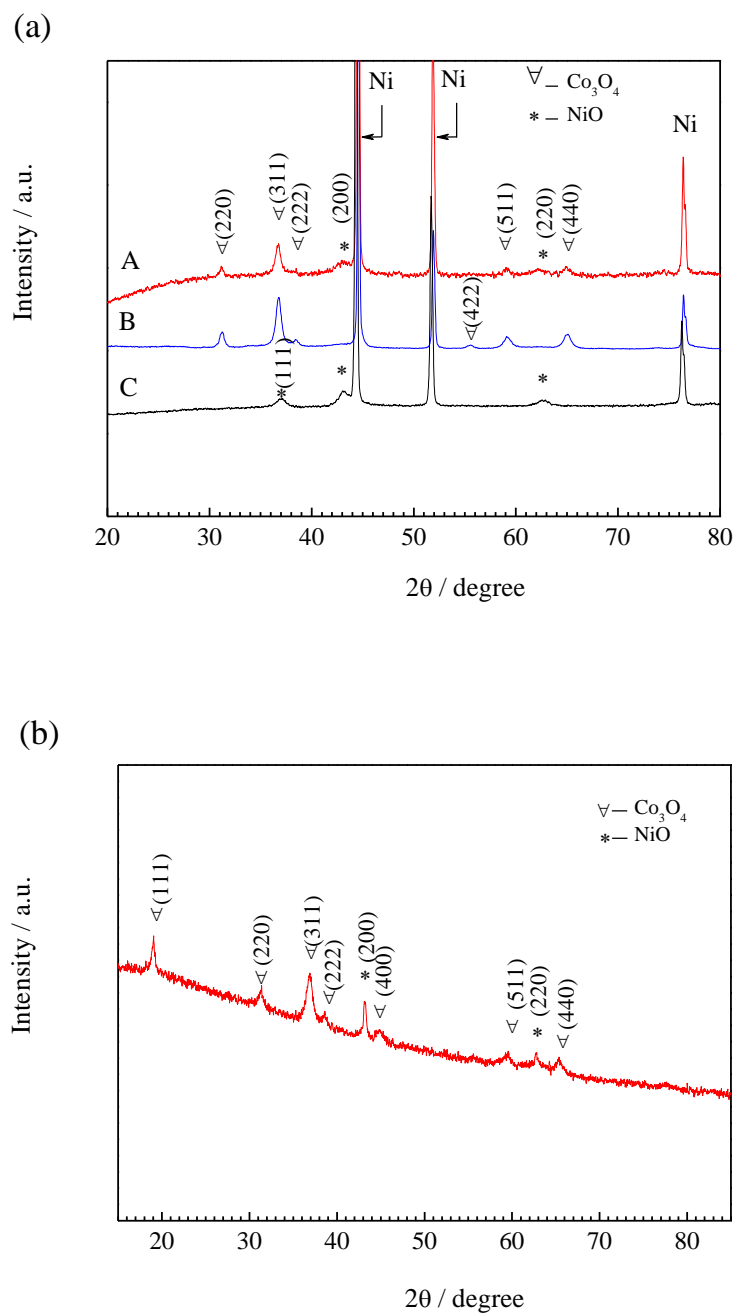


Figure S4. XRD characterization. (a) XRD patterns of (A) $\text{Co}_3\text{O}_4/\text{NiO}$ core/shell nanowire array, (B) Co_3O_4 nanowire array and (C) NiO nanoflake array on nickel foam. (b) XRD pattern of powder of annealed core/shell nanowires scratched from the FTO substrate.

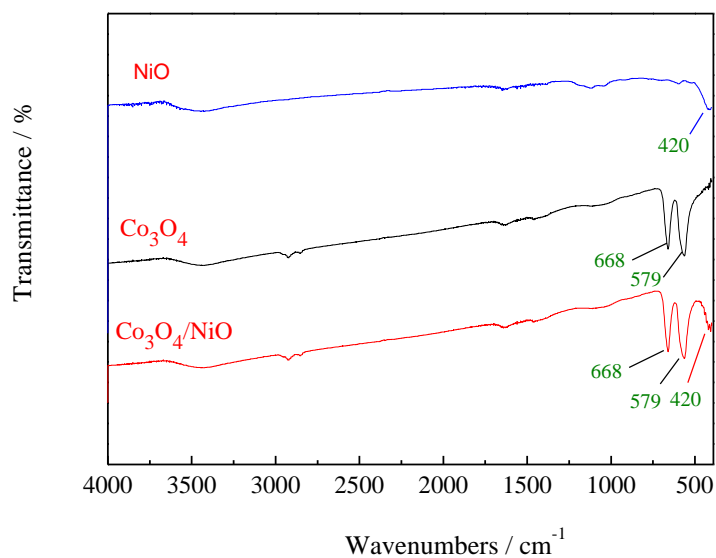


Figure S5. FTIR spectra of $\text{Co}_3\text{O}_4/\text{NiO}$ core/shell nanowire, Co_3O_4 nanowire and NiO nanoflake. Two very strong peaks centered at 668 cm^{-1} and 579 cm^{-1} are characteristic of spinel Co_3O_4 phase. The peak at 420 cm^{-1} is characteristic of NiO phase.

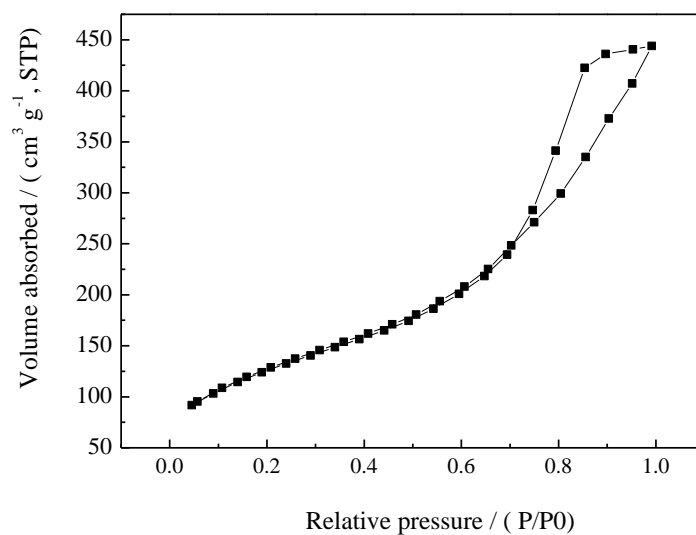


Figure S6. BET measurement of $\text{Co}_3\text{O}_4/\text{NiO}$ core/shell nanowire arrays. The measured surface area is about $415\text{ m}^2/\text{g}$.

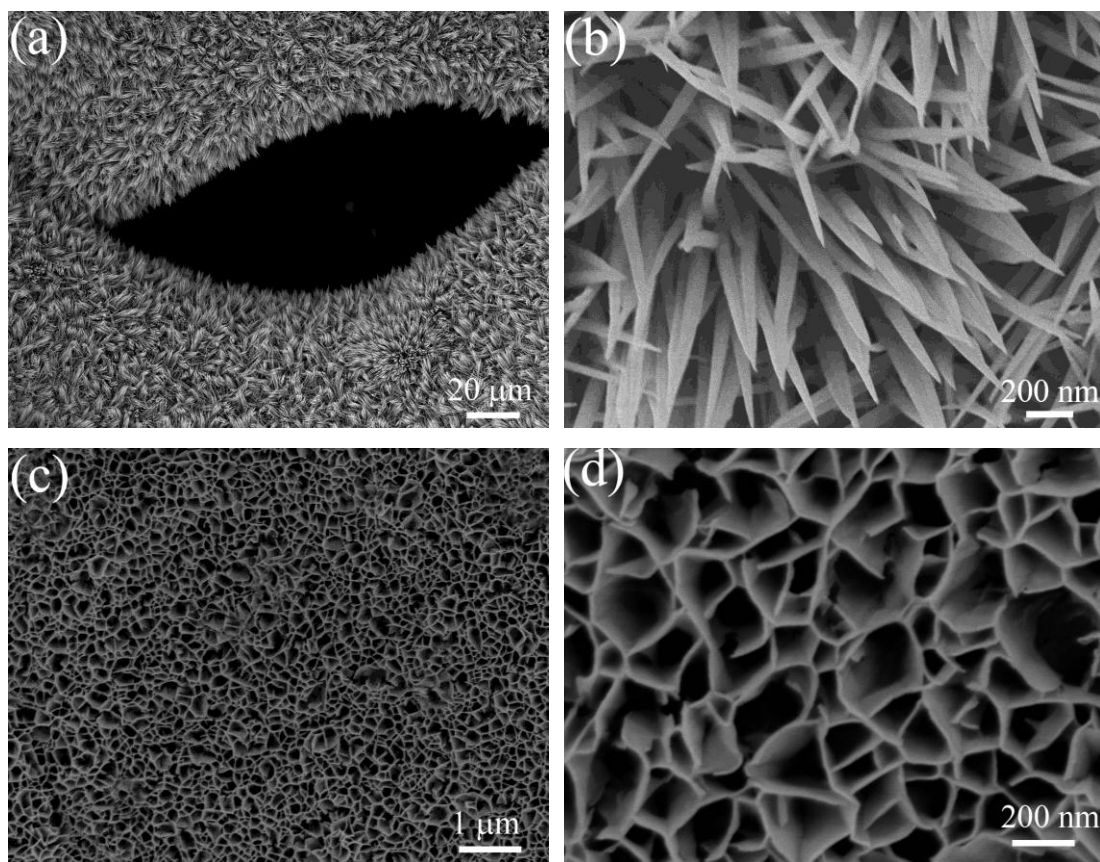


Figure S7. Individual nanostructures. SEM images of (a, b) the Co_3O_4 nanowire arrays and (c, d) NiO nanoflake arrays grown on nickel foam.

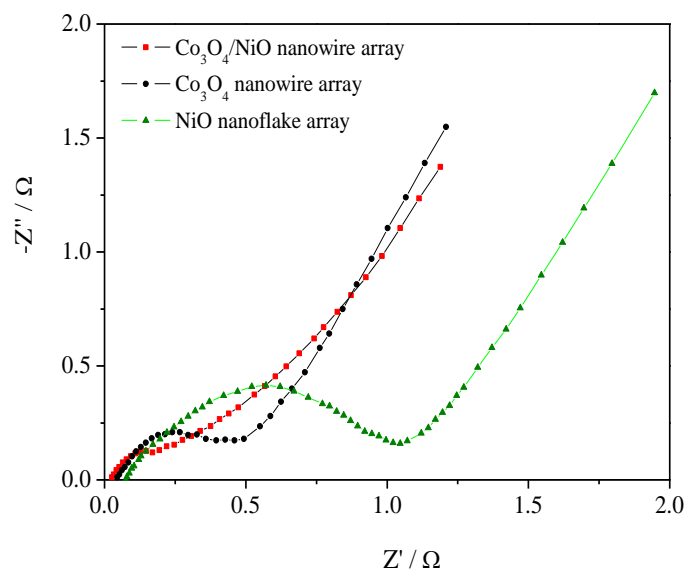


Figure S8. Nyquist plots of three array electrodes with 100 % depth of discharge at the 10th cycle. The substrate is nickel foam.

The impedances of three arrays electrodes all consist of a depressed arc in high frequency regions and a straight slop in low frequency regions. Generally, the semicircle reflects the electrochemical reaction impedance of the film electrode and the straight line indicates the diffusion of the electroactive species. The Co₃O₄/NiO core/shell nanowire arrays exhibit the smallest capacitive arc and lowest slope than the Co₃O₄ nanowire arrays and NiO nanoflake arrays. It is well accepted that bigger semicircle means the larger charge-transfer resistance, and higher slope signifies the faster diffusion rate. It is concluded that the Co₃O₄/NiO core/shell nanowire arrays have the lowest charge transfer resistance and ion diffusion resistance, which is beneficial to the rate capability of the core/shell nanowire arrays.

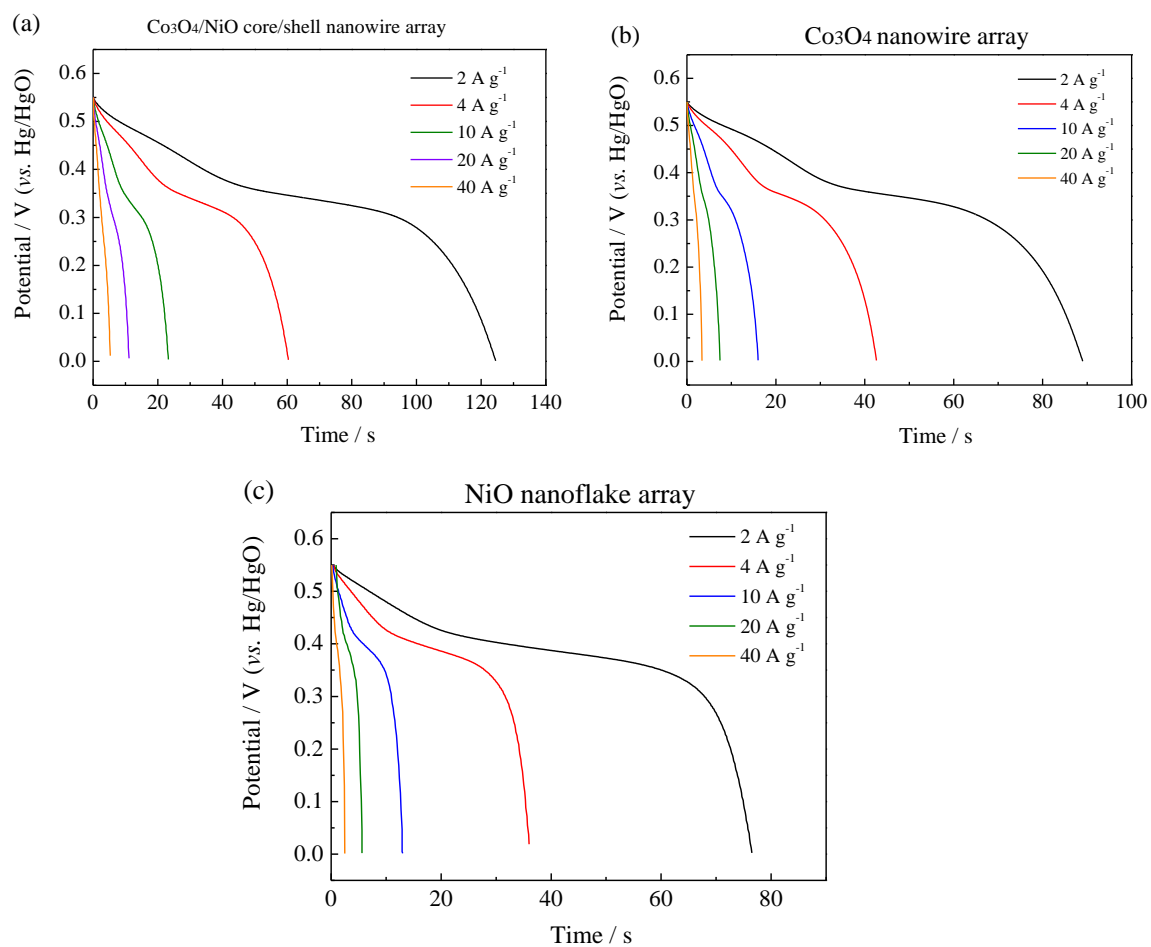


Figure S9. Discharge curves of (a) Co₃O₄/NiO core/shell nanowire arrays, (b) Co₃O₄ nanowire arrays and (c) NiO nanoflake arrays grown on nickel foam at different current densities without activation.

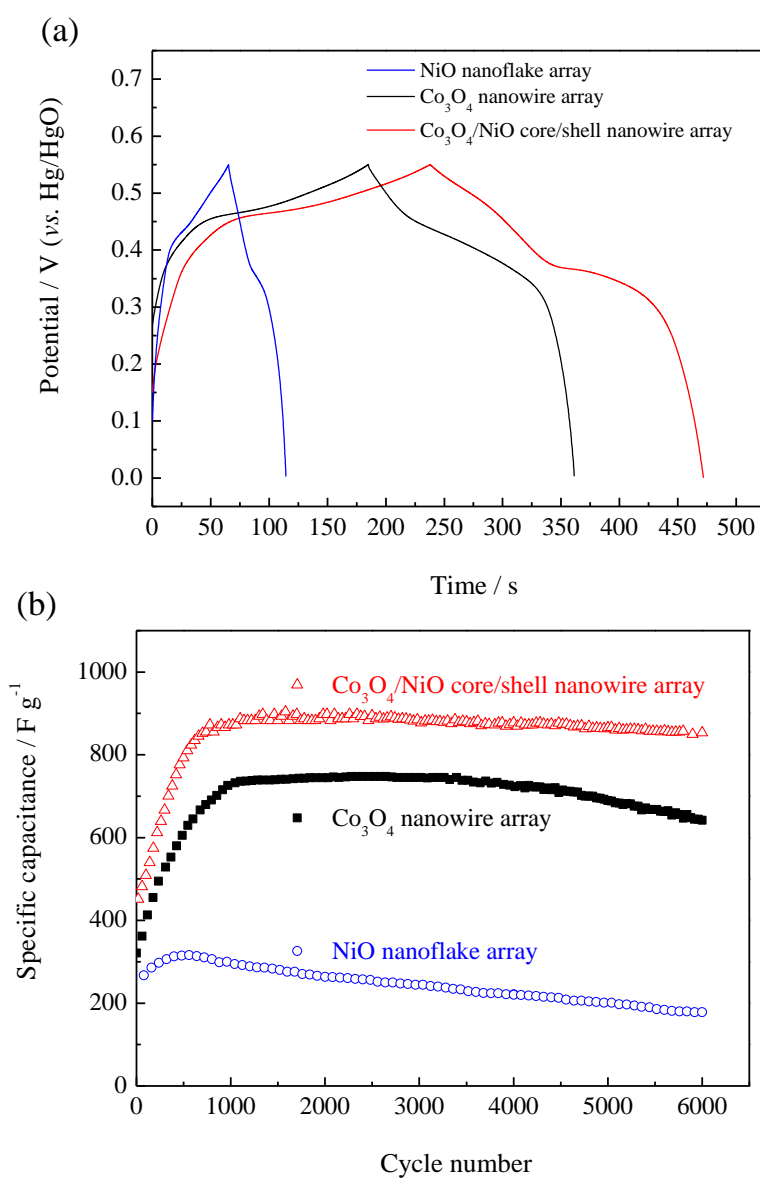


Figure S10. (a) Charge/discharge curves for the three electrodes at the charge/discharge current density of 2 A g^{-1} at the 6000th cycle; (b) Cycling performances of specific capacitances for the three array electrodes at 2 A g^{-1} .

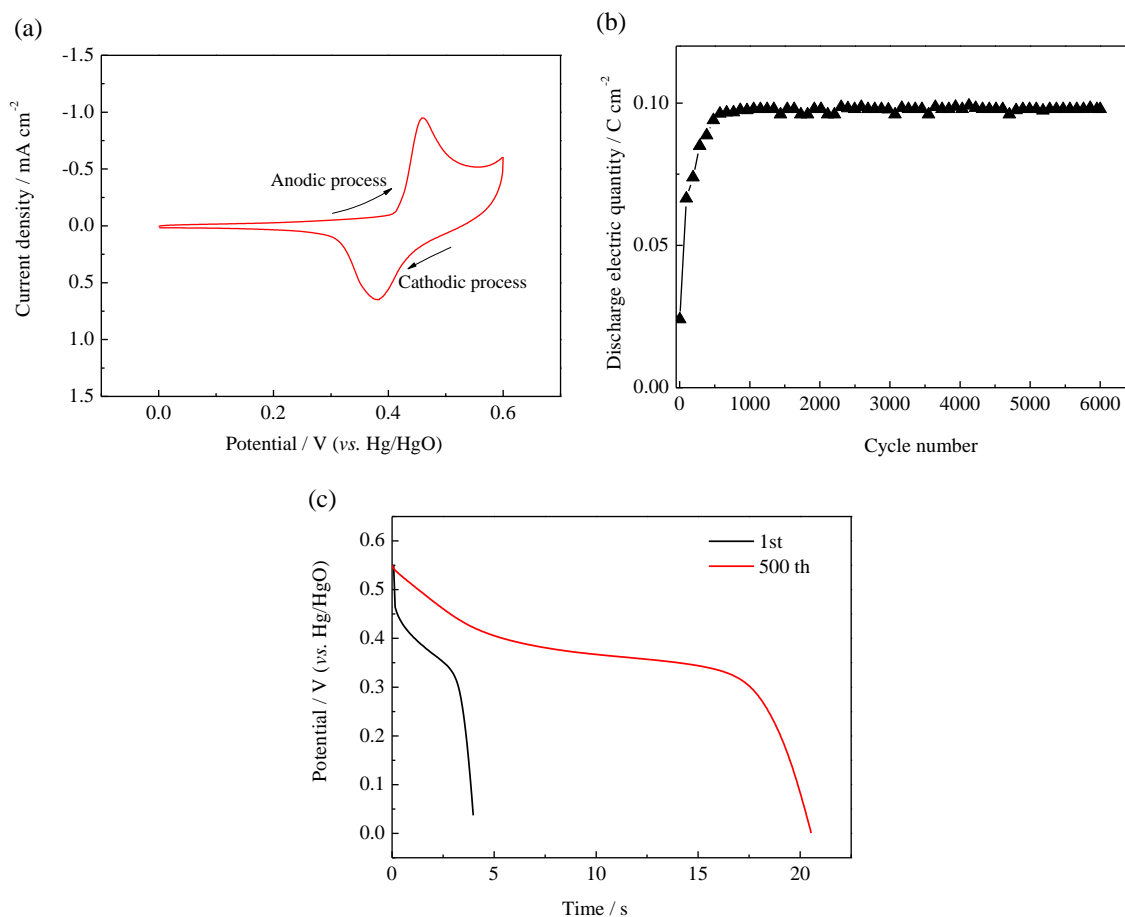


Figure S11. Electrochemical property of nickel foam. (a) CV curve at the scanning rate of 5 mV s⁻¹ at the first cycle; (b) Cycling performance of discharge electric quantity at the current density of 6 mA cm⁻² (corresponding to 2 A g⁻¹ based on mass of Co₃O₄/NiO core/shell nanowire arrays); (c) Discharge curves at 1st and 500th cycles with the current density of 6 mA cm⁻².

Discussion on the contribution of nickel foam It is clearly shown that the nickel foam shows a redox process with low current intensities. This redox couple is attributed to the reversible reaction of Ni(II)/Ni(III) formed on the nickel surface (Figure S11a). Notice that the discharge electric quantity of the nickel foam increases up to about 500 cycles, the remains practically constant (Figure S11b). Its activation process is shorter than those of the Co₃O₄/NiO core/shell nanowire and Co₃O₄ nanowire arrays (take approximately 1000 cycles). As shown in Figure S11c, the nickel foam contributes to the capacitance of the electrode. The discharge time of the nickel foam at 1st and 500th cycle is 3.5 s and 22 s, respectively. It is indicated that the capacitance contribution from the nickel foam increases up to about 500

cycles and keeps stable. **In our case, all specific capacitances are calculated by subtracting the discharge time of nickel foam and reduce the substrate effect to the lowest level.**

Previously, Xing et al. (*J. Power Sources* 196 (2011) 4123) reported the pseudocapacitive performance of the nickel foam and concluded that nickel foam used as the current collector can bring about substantial errors to the specific capacitance values of electrode materials, especially when small amount of electrode active material is used in the measurement. We agree that the nickel foam can contribute to the specific capacitance of the electrode, however, we strongly disagree that the nickel foam is not a suitable substrate for alkaline supercapacitors. Previously, ultrahigh capacitances of nickel/cobalt hydroxide directly electrodeposited on the nickel foam are claimed without subtracting the capacitance of the nickel foam substrate and leads to substantial errors to the specific capacitance values of electrode materials. This phenomenon does exist in some published papers. So long as the contribution of nickel foam is excluded, correct and reasonable specific capacitance values of the active materials can be obtained.

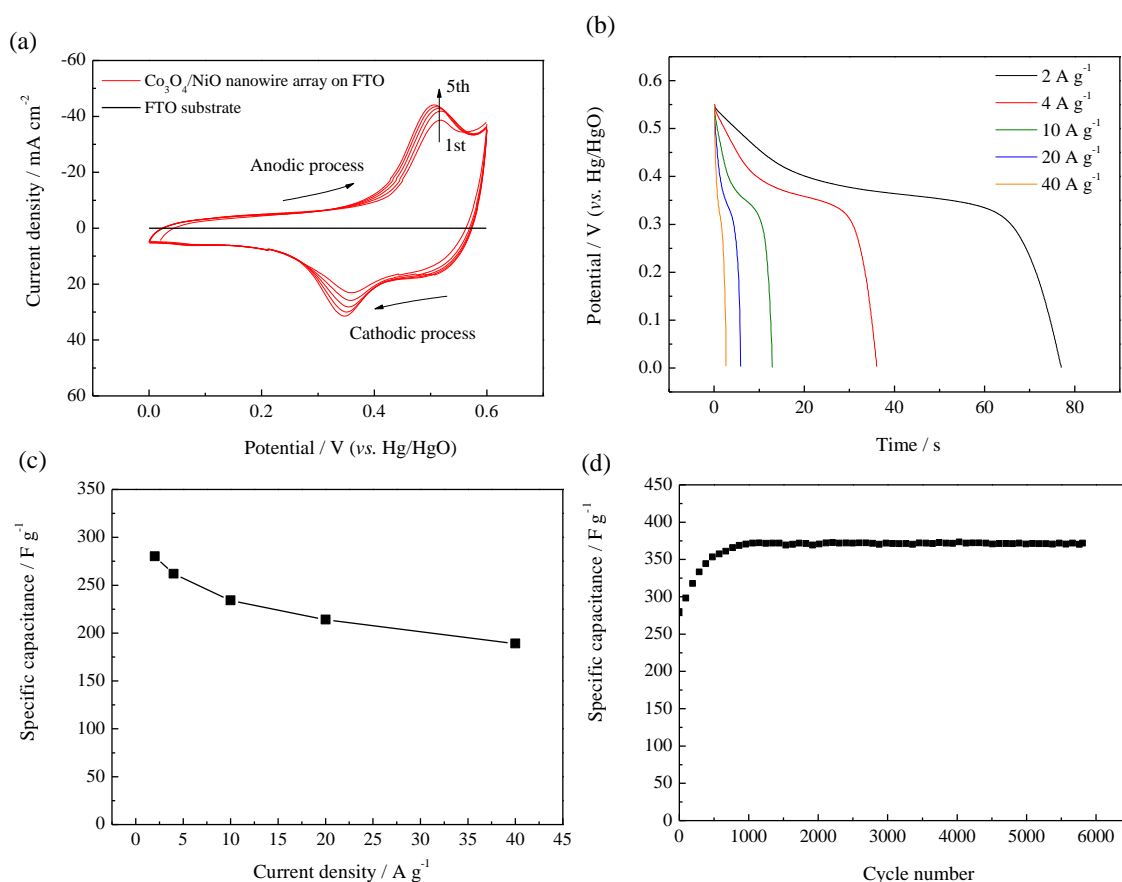


Figure S12. Electrochemical performance of $\text{Co}_3\text{O}_4/\text{NiO}$ core/shell nanowire arrays grown on FTO substrate. (a) CV behavior at the scanning rate of 5 mV s^{-1} . (b) Discharge curves at different current densities, and (c) corresponding specific capacitances; (d) Cycling life at the current density of 2 A g^{-1} .

It is noted that the active material deposited on flat substrate (such as FTO) and 3D porous substrate (nickel foam) exhibits much different electrochemical performance. Figure S12 shows result of the same $\text{Co}_3\text{O}_4/\text{NiO}$ core/shell nanowire arrays but grown on FTO substrate. The increase in anodic and cathodic peak currents in the CV curve indicates that the amount of ions and electrons incorporated into the film increases with cycles. This implies that the reaction activity of the $\text{Co}_3\text{O}_4/\text{NiO}$ core/shell nanowire arrays increases with cycling. In other words, the capacitance increases with the cycling, supported by the cycling performance in Figure S12d. The $\text{Co}_3\text{O}_4/\text{NiO}$ core/shell nanowire arrays grown on the FTO exhibits

pseudocapacitance values (see Figure S12 b and c) that are much lower than those obtained from the nickel substrate. Moreover, the core/shell nanowire arrays on the FTO also take about 1000 cycles to be activated and reach the highest capacitance of 380 F g^{-1} at 2 A g^{-1} . The long activation process is similar to those obtained on the nickel foam. This means the long activation process is intrinsic to the active material rather than substrates. *Taking above together, we do believe that the nickel foam is a good current collector in alkaline supercapacitors as long as we subtract the contribution from the nickel foam to get correct specific capacitances of the active material.*

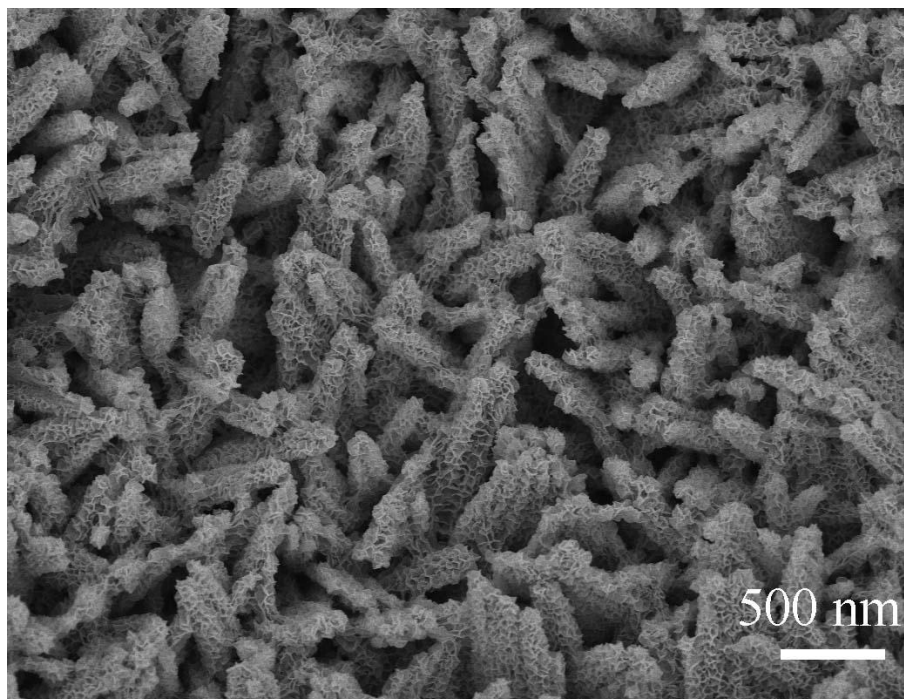


Figure S13 SEM image of $\text{Co}_3\text{O}_4/\text{NiO}$ core/shell nanowire array grown on nickel foam after 6000 cycles at 2 A g^{-1} .

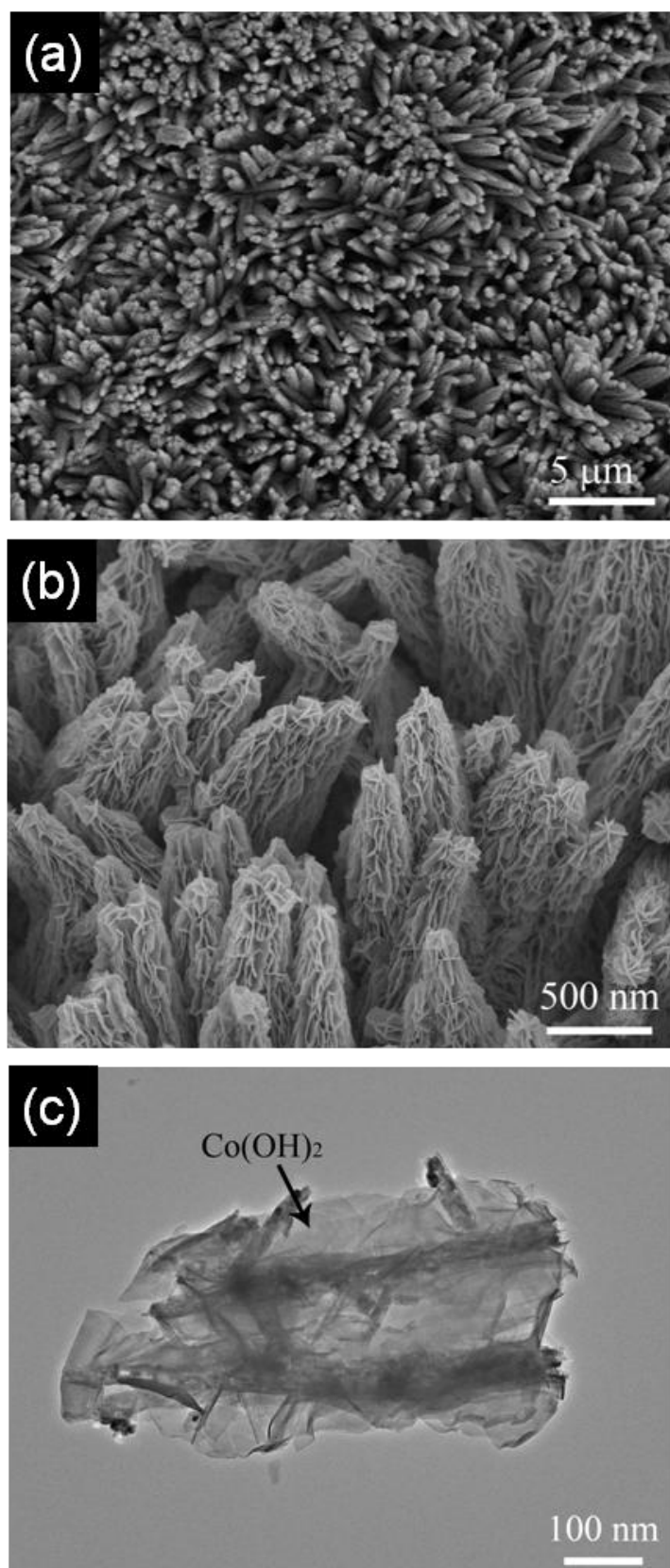


Figure S14 $\text{Co}_3\text{O}_4/\text{Co}(\text{OH})_2$ core/shell nanowire arrays fabricated using similar method.